Electronic Supplementary Material

Marrying luminescent Au nanoclusters to TiO_2 for visible-light-driven antibacterial application

Haiguang Zhu,[†1] Naiwei Liu,[†1] Ziping Wang,[2] Qiang Xue,[1] Qing Wang,[1] Xiaomeng Wang,[1] Yong Liu,[1] Zhengmao Yin,[1] and Xun Yuan[1]*

[1]College of Materials Science and Engineering, Qingdao University of Science and Technology (QUST), 53 Zhengzhou Rd., Shibei District, Qingdao 266042, P. R. China. Email address: yuanxun@qust.edu.cn

[2]Weifang University of Science and Technology, Shandong Peninsula Engineering Research Center of Comprehensive Brine Utilization, Weifang 262700, P. R. China.

[†]These two authors contributed equally to this article

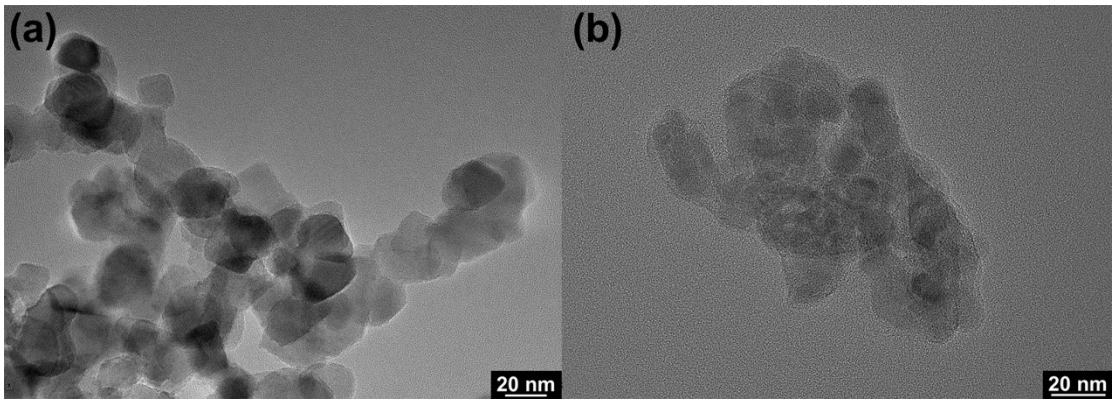

Figure S1. TEM images of TiO_2 nanoparticles before (a) and after (b) amination by APTES.

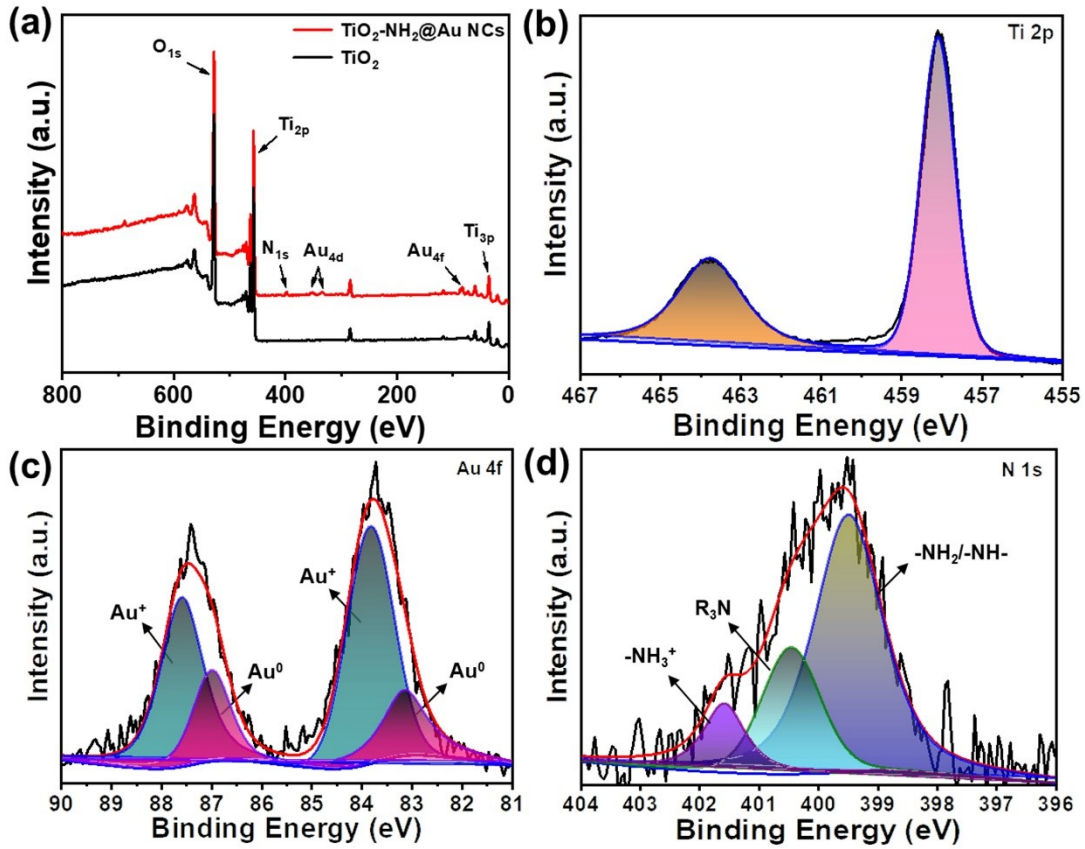

Figure S2. (a) XPS spectra of pristine TiO_2 and TiO_2-NH_2@Au NCs. High-resolution XPS surveys of Ti 2p species (b) of pristine TiO_2, Au 4f species (c) and N 1s species (d) of TiO_2-NH_2@Au NCs.

Supplementary Note I: XPS was performed to analyze the surface composition as well as the chemical valence states of TiO_2 and TiO_2-NH_2@Au NCs. As shown in Figure S2a, the TiO_2-NH_2@Au NCs exhibits a weak signal of N 1s in the wide-scan XPS spectrum comparing with pristine TiO_2, which may be originated from the APTES and GSH. Moreover, two new signals corresponding to Au 4f and Au 4d could be clearly seen in the XPS spectrum of the TiO_2-NH_2@Au NCs, which provides another evidence on the hybridization of Au NCs with the TiO_2. Meanwhile, the high-resolution XPS survey of Ti 2p for pristine TiO_2 (Figure S2b) exhibits two peaks at binding energies of 458.0 and 463.7 eV, corresponding to Ti $2p_{3/2}$ and Ti $2p_{1/2}$, respectively.[1] The peaks

with binding energy of 87.00 eV and 83.10 eV in Figure S2c are ascribed to the Au $4f_{5/2}$ and Au $4f_{7/2}$ of metallic Au (Au^0), respectively. By contrast, the additional doublet peaks at 87.80 eV and 83.80 eV are assigned to the Au $4f_{5/2}$ and Au $4f_{7/2}$ of Au^+, respectively (Figure S2c).[2-4] In addition, the high-resolution N 1s spectrum of the TiO_2-NH_2@Au NCs could be deconvoluted to three components at 399.51, 400.79, and 401.63 eV (Figure S2d), which can be attributed to the $-NH_2/-NH-$, R_3N and $-NH_3^+$ functional groups, respectively.[5] As a result, it confirms the successful grafting of Au NCs on the surface of TiO_2-NH_2.

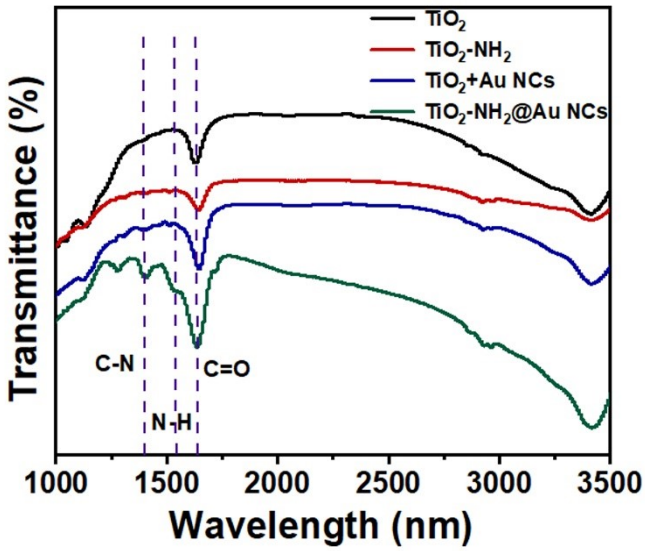

Figure S3. FTIR spectra of TiO_2, TiO_2-NH_2, TiO_2+Au NCs, and TiO_2-NH_2@Au NCs.

Supplementary Note II: As comparing with the FTIR spectra of TiO_2, TiO_2-NH_2 and TiO_2+Au NCs, the FTIR spectrum of TiO_2-NH_2@Au NCs displays three peaks at 1640 cm^{-1}, 1540 cm^{-1}, and 1400 cm^{-1}, corresponding to C=O stretching, N−H bending, and C−N stretching, respectively.[6] This result further proves that the TiO_2 and Au NCs are linked together by the amidation reaction.

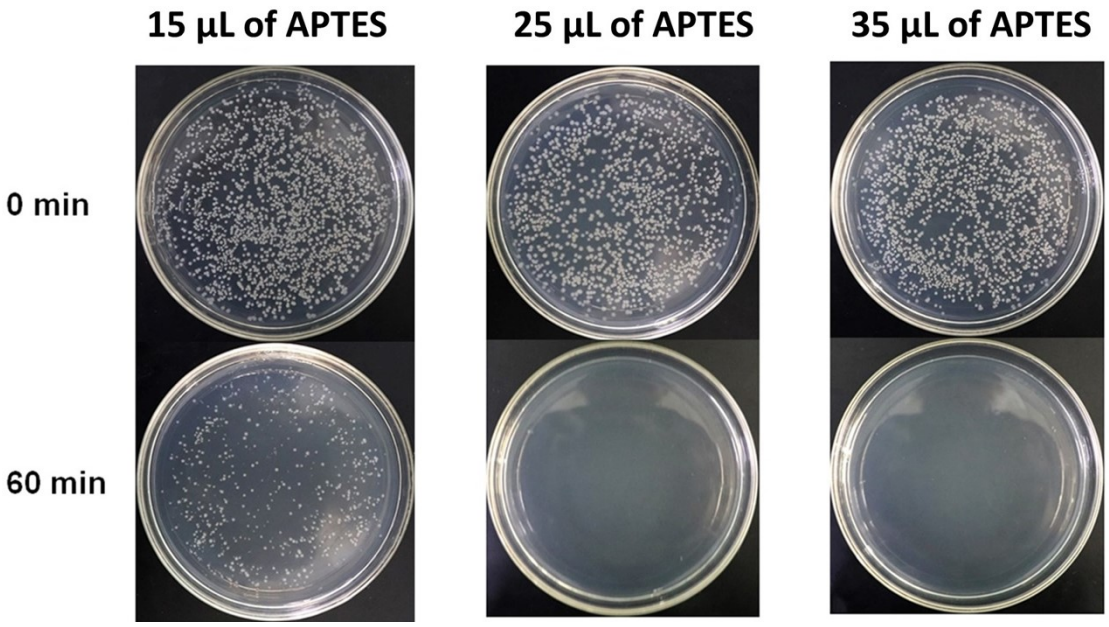

Figure S4. Bacterial colony growth of *E. coli* in presence of three samples of TiO_2-NH_2 @Au NCs prepared with the APTES dosage of 15, 25, and 35 µL.

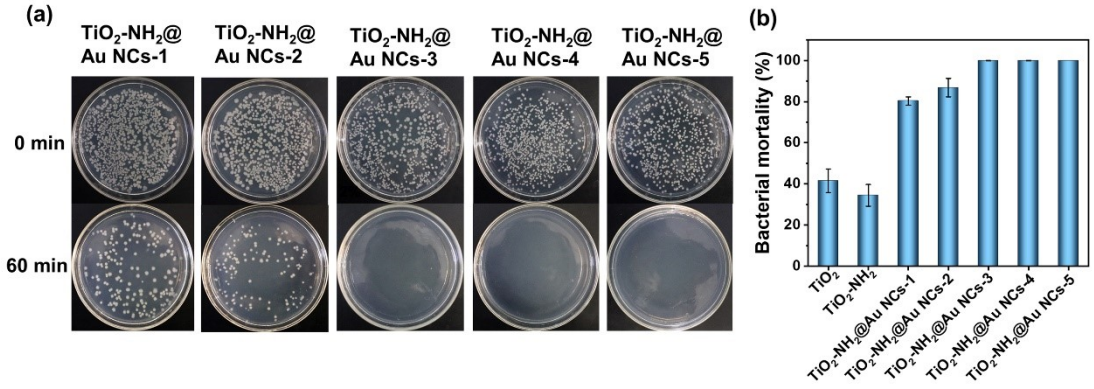

Figure S5. (a) Bacterial colony growth of *E. coli* in presence of five samples of TiO_2-NH_2@Au NCs with different loadings of Au NCs. (b) The antibacterial rates of TiO_2-NH_2@Au NCs-X photocatalysts as well as other reference samples such as TiO_2 and TiO_2-NH_2. (Note: X = 1, 2, 3, 4 and 5, which correspond to samples with different concentrations of the loaded Au NCs from 4 mM, 8 mM, 12 mM, 16 mM, and 20 mM, respectively).

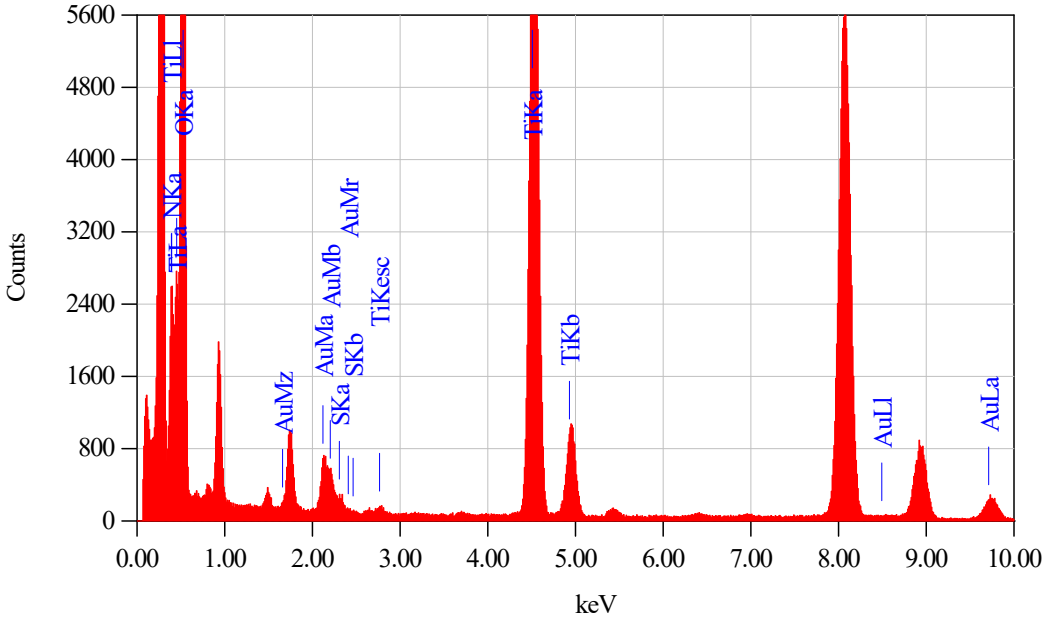

Figure S6. EDX spectrum of the TiO_2-NH_2@Au NCs prepared at the optimal concentration of Au NCs (i.e., 12 mM).

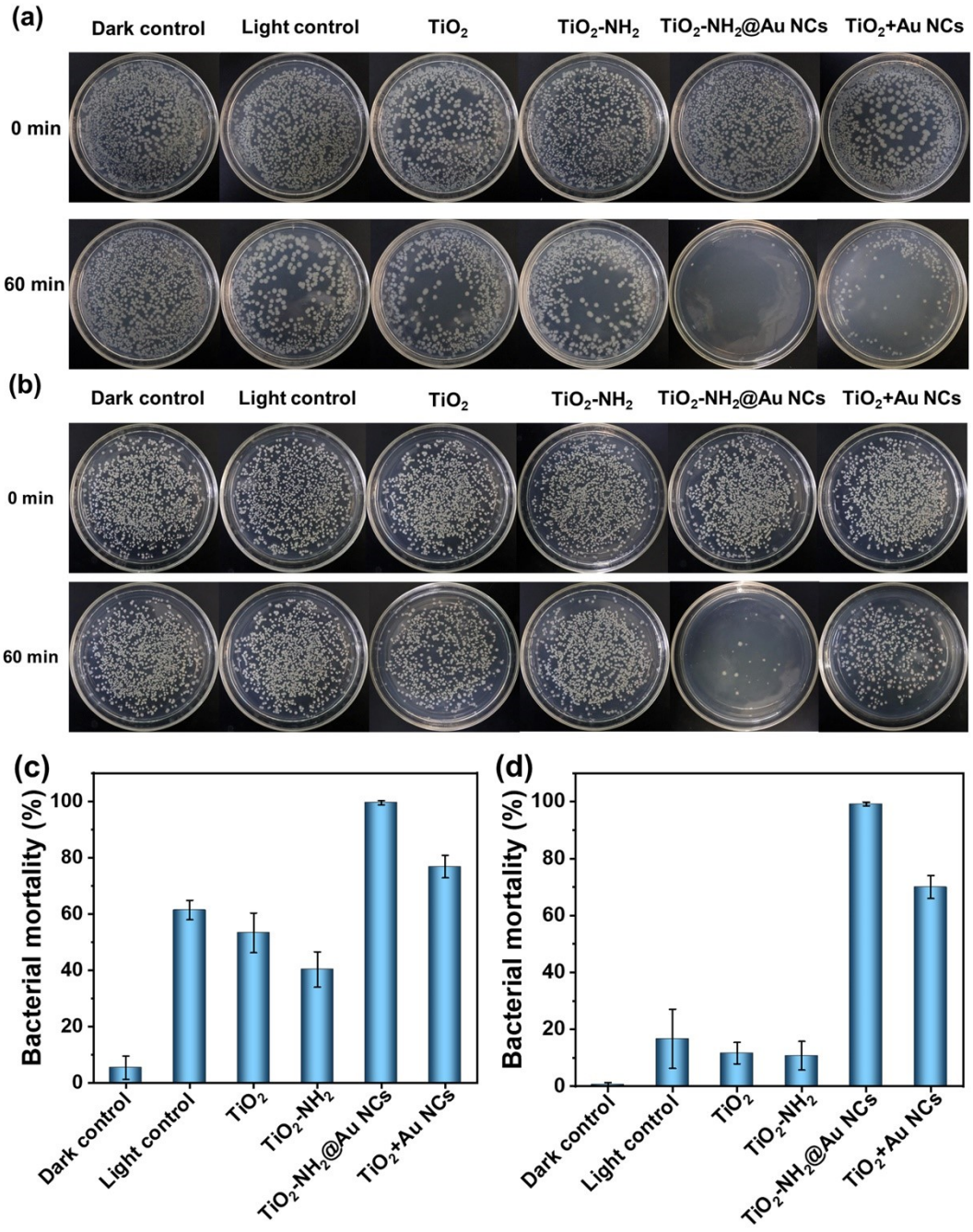

Figure S7. Bacterial colony growth of *B. subtilis* (a) and *P. aeruginosa* (b) in the presence of TiO_2, TiO_2-NH_2, TiO_2-NH_2@Au NCs, TiO_2+Au NCs under either visible light illumination or dark condition for 60 min. Bactericidal activity for gram-positive *B. subtilis* (c) and gram-negative *P. aeruginosa* (d) under different conditions.

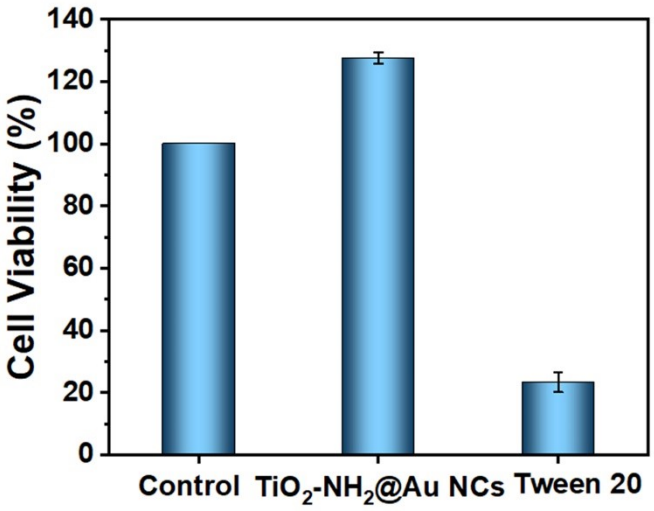

Figure S8. Cytotoxicity assay of TiO_2-NH_2@Au NCs with the same dosage of HeLa cells evaluated by MTT Kit after 24 h treatment.

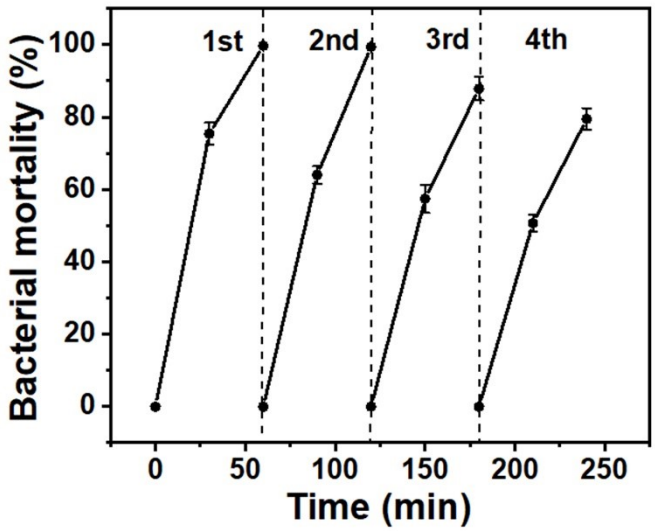

Figure S9. Durability test of the TiO_2-NH_2@Au NCs for visible-light-driven bacterial killing of *E. coli.*

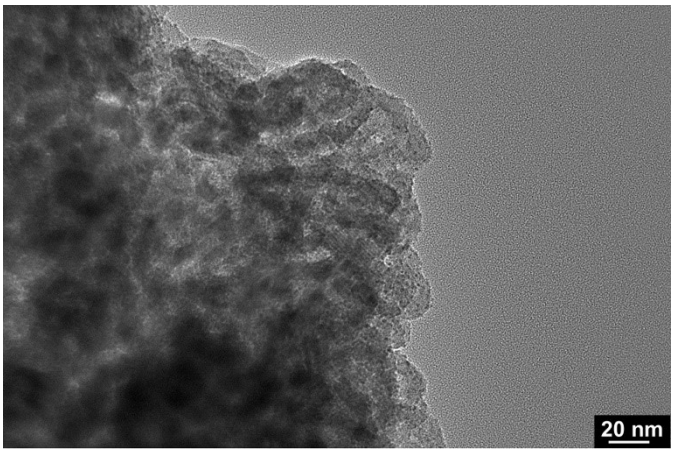

Figure S10. TEM image of the TiO_2-NH_2@Au NCs after photocatalytic test.

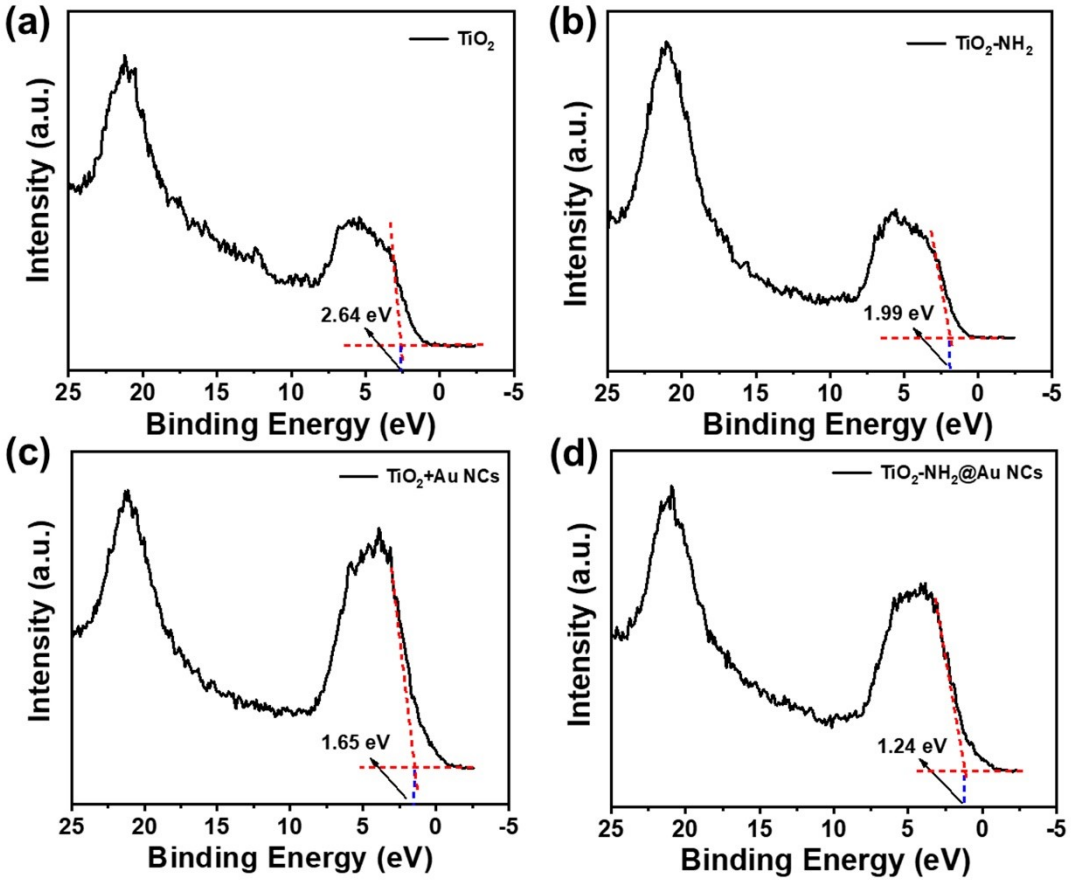

Figure S11. VB-XPS curves of TiO_2 (a), TiO_2-NH_2 (b), TiO_2+Au NCs (c) and TiO_2-NH_2@Au NCs (d).

Supplementary Note III: From the VB-XPS plots, the VB potentials of TiO_2, TiO_2-NH_2, TiO_2+Au NCs and TiO_2-NH_2@Au NCs ($E_{VB\text{-}XPS}$) were measured as 2.64, 1.99, 1.65 and 1.24 eV according to their VB-XPS plots, respectively. Therefore, the VB

values (vs. NHE) of TiO_2, TiO_2-NH_2, TiO_2+Au NCs and TiO_2-NH_2@Au NCs were calculated to be 2.70, 2.05, 1.71 and 1.30 eV, respectively, based on the formula $E_{NHE} = \varphi + E_{VB\text{-}XPS} - 4.44$ (E_{NHE}: standard hydrogen electrode potential; φ: electron work function of the XPS analyzer, and the value was 4.50.).[7, 8] The CB position can be deduced from the equation, $E_{CB} = E_{VB} - E_g$ (E_g is the energy bandgap). On the basis of the above equations, the CB positions of TiO_2, TiO_2-NH_2, TiO_2+Au NCs and TiO_2-NH_2@Au NCs were calculated to be -0.50, -1.11, -1.38 and -1.45 eV, respectively.

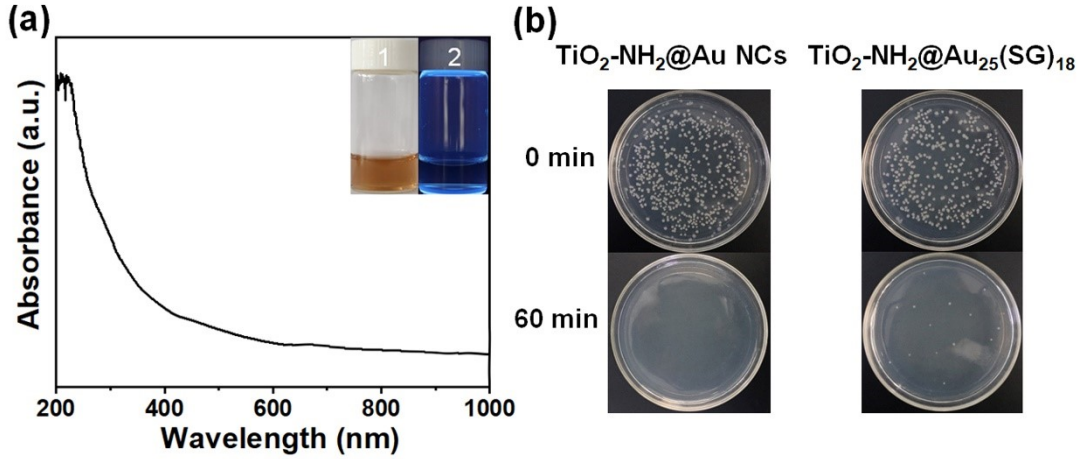

Figure S12. (a) UV−visible absorption spectra of $Au_{25}(SG)_{18}$. The inset show digital photos of the $Au_{25}(SG)_{18}$ solution under (1) visible and (2) UV light irradiation. (b) Bacterial colony growth of *E. coli* in the presence of TiO_2-NH_2@Au NCs and TiO_2-NH_2@ $Au_{25}(SG)_{18}$ under visible light illumination for 60 min.

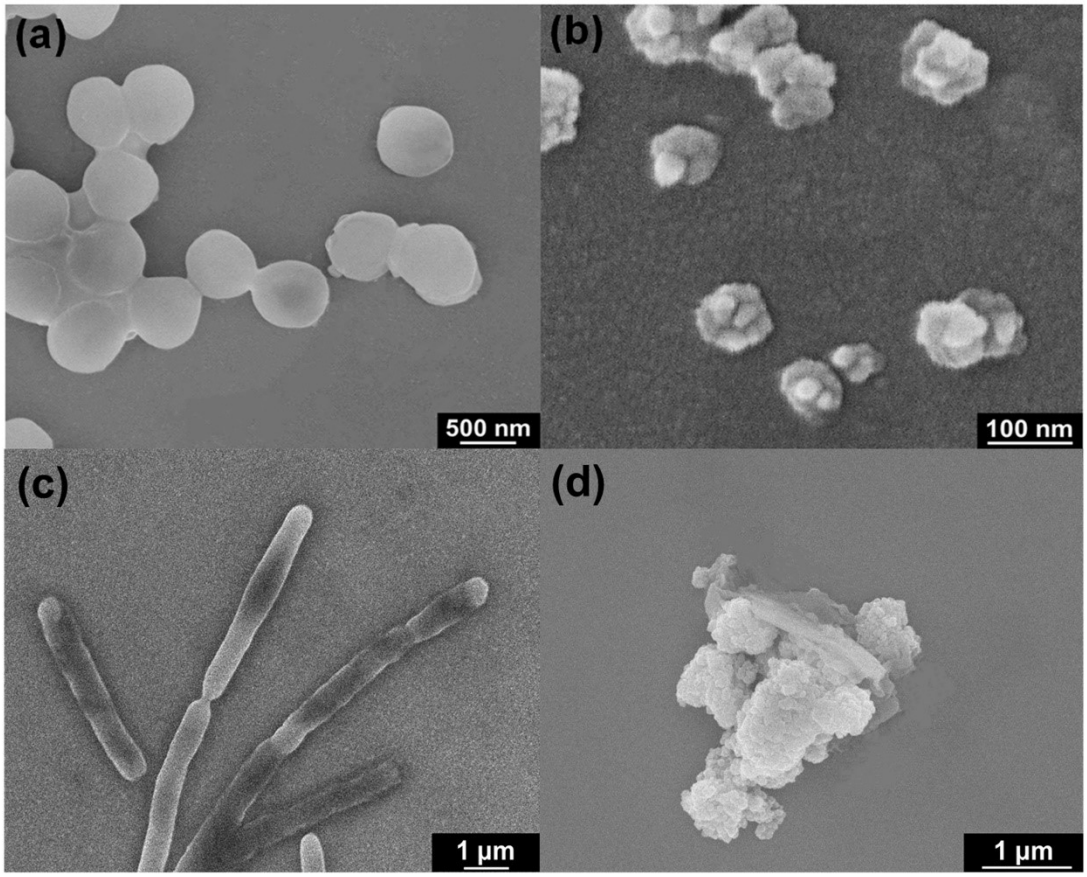

Figure S13. Typical SEM images of bacteria before (a, c) and after (b, d) visible light illumination for 60 min over TiO_2-NH_2@Au NCs. S. aureus: (a, b); E. coli: (c, d).

Reference

1. F.-X. Xiao, Z. Zeng and B. Liu, *J. Am. Chem. Soc.*, 2015, **137**, 10735-10744.
2. Y.-S. Chen, H. Choi and P. V. Kamat, *J. Am. Chem. Soc.*, 2013, **135**, 8822-8825.
3. Y.-S. Chen and P. V. Kamat, *J. Am. Chem. Soc.*, 2014, **136**, 6075-6082.
4. Z. Luo, X. Yuan, Y. Yu, Q. Zhang, D. T. Leong, J. Y. Lee and J. Xie, *J. Am. Chem. Soc.*, 2012, **134**, 16662-16670.
5. Z. Zeng, Y.-B. Li, S. Chen, P. Chen and F.-X. Xiao, *J. Mater. Chem. A*, 2018, **6**, 11154-11162.
6. B. Tamami and H. Yeganeh, *Eur. Polym. J.*, 2002, **38**, 933-940.
7. J. Yuan, X. Liu, Y. Tang, Y. Zeng, L. Wang, S. Zhang, T. Cai, Y. Liu, S. Luo, Y. Pei and C. Liu, *Appl. Catal. B: Environ.*, 2018, **237**, 24-31.
8. J. Xiong, X. Li, J. Huang, X. Gao, Z. Chen, J. Liu, H. Li, B. Kang, W. Yao and Y. Zhu, *Appl. Catal. B: Environ.*, 2020, **266**, 118602.